Numerical Studies of Divertor Conditions at DIII-D Under the Influence of Resonant Magnetic Perturbations

H. Frerichs,[1] O. Schmitz,[1] D. Reiter,[1] T.E. Evans,[2] and Y. Feng[3]
[1)] *Institute of Energy and Climate Research - Plasma Physics, Forschungszentrum Jülich GmbH, Association EURATOM-FZJ, Partner in the Trilateral Euregio Cluster, Jülich, Germany*
[2)] *General Atomics, San Diego, California, CA, USA*
[3)] *Max-Planck Institute for Plasma Physics, Greifswald, Germany*

(Dated: 7 May 2012)

The impact of resonant magnetic perturbations on the edge plasma, in particular on the target heat flux, are investigated with the EMC3-EIRENE code. The focus is on recent model advancements, such as neutral gas pumping and re-fuelling and a modification of the magnetic field structure by plasma response effects, as well as on the issue of corrections to the parallel electron heat conductivity at low collisionalities and impurity radiation. Finally, we study toroidally averaged target profiles.

PACS numbers: 52.25.Fi, 52.55.Rk, 52.65.-y, 52.65.Kj
Keywords: plasma edge transport, magnetic perturbations, computer simulations

I. INTRODUCTION

Resonant magnetic perturbations (RMPs) are a promising candidate for the control of edge localized modes (ELMs) in ITER according to successful demonstrations at present machines[1–3]. At the DIII-D tokamak already now the study of ITER similar shape plasmas in the presence of RMPs is carried out. Such scenarios are also investigated numerically with the EMC3-EIRENE code[4,5], which is a coupled 3D Monte Carlo transport code for the edge plasma (fluid transport model) in interaction with neutral particles (a 3D kinetic transport model). The classical transport model by Braginskii[6] is applied for plasma transport along magnetic field lines, while anomalous cross-field transport is taken into account by a diffusion ansatz with free model parameters for the diffusion coefficients.

The 3D magnetic field structure, with or without RMP screening effects, is provided as input for the code: a field aligned grid is used for a fast reconstruction of magnetic field lines during transport simulations[7,8]. A first comparison has been carried out between the vacuum RMP field configuration and an 'ad hoc' plasma response configuration with complete screening of corresponding modes on selected rational flux surfaces[9]. Furthermore, the EMC3-EIRENE code has been advanced to include a more realistic treatment of gas flow and recycling dynamics in the divertor: pumping of neutral gas from the divertor region by separating target recycling and pumping locations, as well as gas re-fuelling in other locations[10].

In the present contribution we combine these two recent studies and model advancements and focus on remaining model uncertainties. Recent simulations for RMP H-mode plasmas at DIII-D have shown a significant striation pattern in both particle and heat fluxes to the divertor target[11], but such a strong heat flux striation is not observed in the corresponding experiment[12]. Furthermore, a strong temperature reduction at the plasma edge by RMPs is found in simulations[10] but not in the experiment. These plasma discharges are characterized by a low diverotor density and low collisionality, which suggests that kinetic corrections to the parallel electron heat conduction are probably necessary.

We begin with an analysis of the impact of an 'ad hoc' limited parallel electron heat conductivity, and continue with the effects of neutral gas pumping, impurity radiation and an 'ad hoc' plasma response to the RMP field. Finally, we study the toroidally averaged target heat flux, which is of interest e.g. for fast rotating RMP fields.

II. TARGET HEAT FLUX STUDIES

The following analysis is based on the ITER similar shape DIII-D discharge 132741 at 3760 ms. This discharge is characerized by the following parameters:

toroidal magnetic field	$B_t = 1.8\,\mathrm{T}$
plasma current	$I_p = 1.5\,\mathrm{MA}$
effective input power	$P_{\mathrm{in}} = 6.3\,\mathrm{MW}$
elongation	$\kappa \approx 1.8$
average triangularity	$\delta \approx 0.5$
edge safety factor	$q_{95} = 3.52$
perturabtion current	$I_c = 4\,\mathrm{kA}$

The perturbation field is provided by a set of six upper and lower rectangular coils located at the low field side of the machine. A configuration with even parity and toroidal mode number $n = 3$ is used. An overview of the magnetic configuration with vacuum RMP field is given in figure 1 (a) and (d).

Boundary conditions for the transport code are the effective input power P_{in} (see table above) and the steady state pumping and re-fuelling rate $\Gamma_{\mathrm{in/out}} = 1.12 \times 10^{21}\,\mathrm{s}^{-1}$. Coefficients for anomalous particle, momentum and energy cross-field transport are set to $D_\perp =$

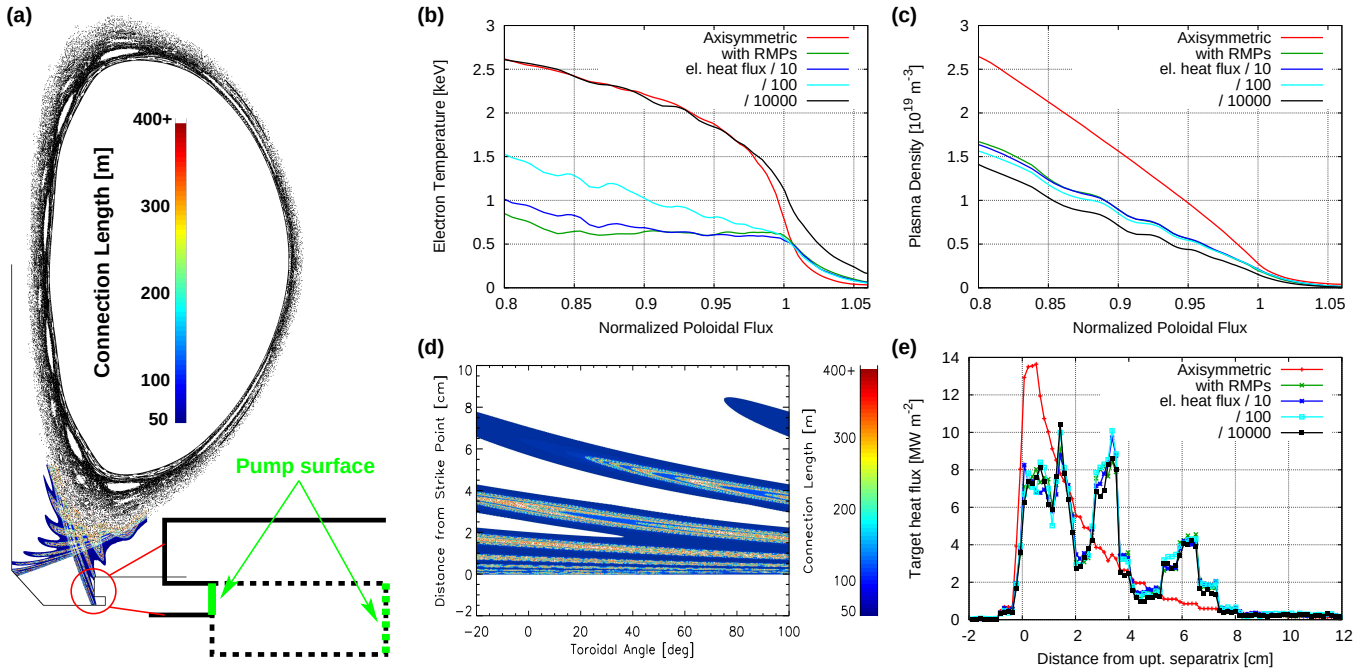

FIG. 1. (a) Poincaré plot of DIII-D discharge 132741. The wall-to-wall connection length L_c of magnetic field lines in the divertor region is color-coded. Pumping of neutral gas is taken into account by a pump surface (solid). An alternative implementation with an extended pump plenum is sketched by the dashed lines. (b), (c) Midplane profiles of electron temperature and plasma density. (d) Magnetic footprint at the inner strike point (ISP). (e) Target heat flux at the ISP at $\varphi = 0\,\mathrm{deg}$.

$0.2\,\mathrm{m^2\,s^{-1}}$, $\eta_\perp = m_i\, n_i\, D_\perp$ and $\chi_{e\perp} = \chi_{i\perp} = 0.6\,\mathrm{m^2\,s^{-1}}$. The pumping quality (i.e. the pump probability of particles crossing the pump-surface) is set to $\eta_{\mathrm{pump}} = 0.75$.

A. Limited parallel el. heat conduction

In order to estimate the effect of a reduction of the parallel electron heat conductivity $\kappa_\parallel^e$ at low collisionalities, we introduce an 'ad hoc' limiting factor $\beta_\parallel$ in the effective heat conductivity $\kappa_\parallel^{e*} = \beta_\parallel \cdot \kappa_\parallel^e$. This factor can easily be introduced in a Monte Carlo scheme. On the other hand, a limiting factor obtained from a free streaming limit

$$\beta_\parallel = \left(1 + \frac{\kappa_\parallel^e\,|\nabla_\parallel T_e|}{\alpha_e\, n_e\, v_{th}\, T_e}\right)^{-1}$$

requires the calculation of gradients of intrinsically (Monte Carlo) noisy data besides introducing a free model parameter α_e as well.

The impact of a constant reduction by 1, 2 and 4 orders of magnitude on the midplane profiles of electron temperature T_e and plasma density n is shown in figure 1 (b) and (c), respectively. It can be seen that it takes at least a reduction of 2 orders of magnitude to find a significant impact on T_e. If $\kappa_\parallel^e$ is reduced by 4 orders of magnitude, then the strong 'energy pump-out' by the fast parallel transport is suppressed and T_e is restored up to the axisymmetric level. As a side effect, the sound speed is increased which results in an increase of parallel particle transport and a weak reduction of plasma density. However, despite the strong impact on the electron temperature, there is no impact on the target heat flux q_t. This is demonstrated in figure 1 (e) by profiles of q_t in comparison to that of the axisymmetric configuration.

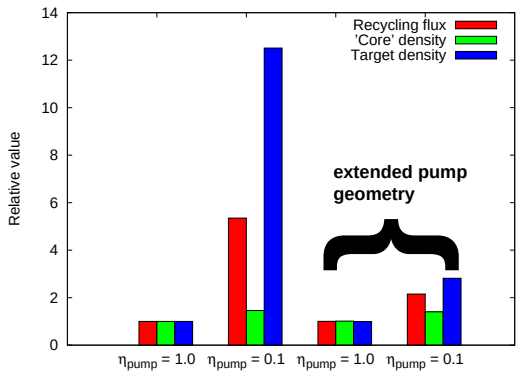

FIG. 2. Impact of the pumping quality η_{pump} and geometry normalized to $\Gamma_{\mathrm{rec}} = 2.05\,\mathrm{kA}$, $n_{\mathrm{core}} = 1.8 \cdot 10^{19}\,\mathrm{m^{-3}}$ and $n_{\mathrm{div}} = 1.2 \cdot 10^{18}\,\mathrm{m^{-3}}$.

B. Neutral gas pumping

While a reduction of the pumping quality η_{pump} has a significant impact on the recycling flux and consequently

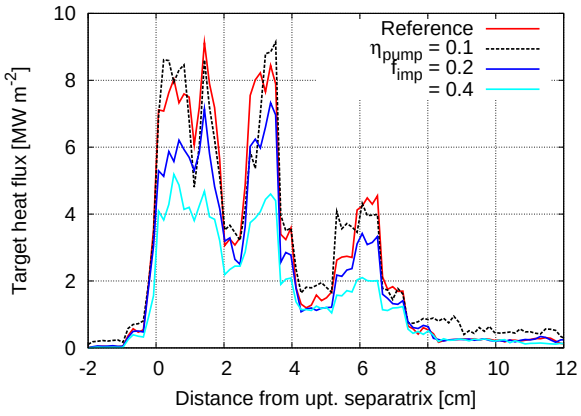

FIG. 3. Target heat flux at $\varphi = 0$ deg for lower pumping quality and with impurity radiation (20 % and 40 % of $P_{\rm in}$).

on the density in the divertor as well as upstream (see figure 2), we have found no impact on the target heat flux (compare red and black dashed lines in figure 3 (a))). Furthermore, we find that if we take into account a larger part of the pump plenum (dashed lines in figure 1 (a)), the impact of the parameter $\eta_{\rm pump}$ is mitigated (see figure 2), in particular the same results are found for $\eta_{\rm pump} = 1.0$. Hence, we conclude that a moderately high value of $\eta_{\rm pump}$ is closest to reality and we stick to the originial pumping geometry which requires much less computational effort.

C. Impurity radiation

We take into account local impurity radiation $P_{\rm imp}$ from sputtered carbon within a simple Corona model. The impurity density is taken to be proportional to the main ion density with a factor determined by a prescribed impurity radiation fraction $f_{\rm imp}$ so that:

$$\int dV\, P_{\rm imp} \;=\; f_{\rm imp}\, P_{\rm in}.$$

The impact on the target heat flux is shown in figure 3 (a). It can be seen that the complete profile is reduced by the same amount of impurity radiation, i.e. there is no redistribution of heat flux from the outer to the inner peak. Further studies which include the production process and transport of impurities are ongoing.

D. Plasma response

An 'ad hoc' plasma response to an externally applied RMP field is taken into account by a helical current sheets[9,13]. These current sheets are located at a selected set of magnetic flux surfaces and are tuned for an optimal

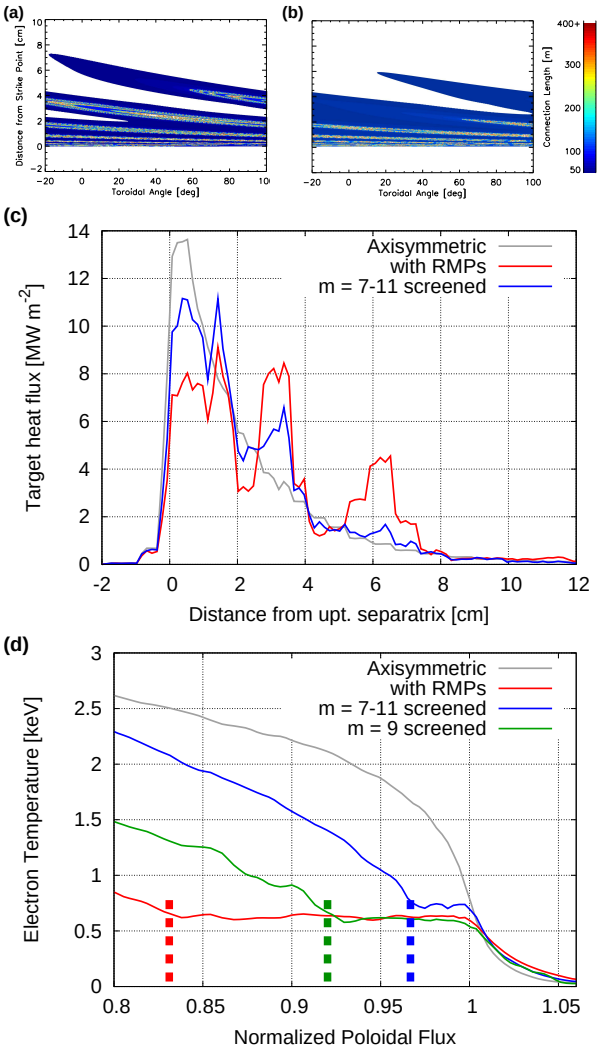

FIG. 4. Magnetic footprint at the ISP with screening (a) at the $m = 9$ surface and (b) at the $m = 7 - 11$ surfaces. (c) Target heat fluxes and (d) radial midplane profiles of T_e at the LFS for these configurations. The dashed lines mark the beginning of the region in which field lines connect to the target within a few el. mean free paths.

screening of the corresponding modes of the externally applied field on these surfaces.

We study two response cases: screening on a single resonant surface with poloidal mode number $m = 9$ and screening on the $m = 7 - 11$ surfaces. The size of the magnetic footprint diminishs with increasing screening, which is demonstrated in figure 4 (a) and (b), and the radial extent of the open field line region is reduced as well[9]. This modification is reflected in the target heat flux (which is shown in part (c)): the secondary peaks shrink while the primary one increases towards the axisymmetric limit. The impact on the target particle flux is similar but weaker due to a broader axisymmetric base profile[9]. The strong 'energy pump-out' effect found in the

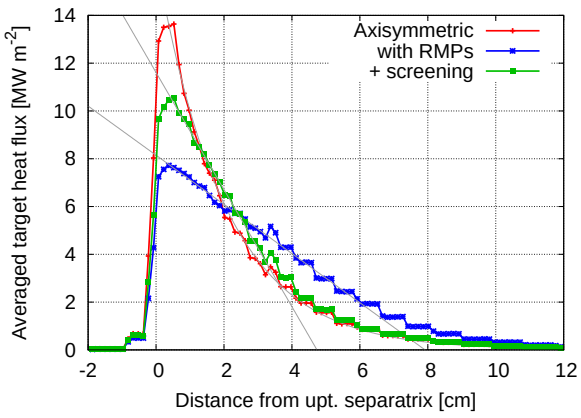

FIG. 5. Toroidally averaged target heat flux profiles for RMP configurations with and without screeing compared to the axisymmetic configuration.

vacuum configuration is reduced (figure 4 (d)), however, a flat T_e profile remains in the respective open field line region (which is related to the large $\kappa_{\|}^e$). Furthermore, the 'particle pump-out' effect (which is indeed observed experimentally) is reduced as well, therefore we conclude that screening cannot be too strong, also because of clear experimental evidence regarding particle flux strike point splitting.

E. Averaged heat flux profiles

An important issue of RMP application is also the modification of the toroidally averaged target heat flux

$$\overline{q}_t(L) \;=\; \frac{1}{2\,\pi}\int_0^{2\,\pi} d\varphi\, q_t(\varphi, L), \qquad (1)$$

where L is the coordinate along the axisymmetric wall in the R-Z plane, starting from the unperturbed separatrix strike point. The target heat flux in the axisymmetric configuration is characterized by an exponential decay $\overline{q}_t \;=\; q_{t0}\,\exp\left(-L/\lambda\right)$. A fit to the simulation results allows to determine the e-folding length:

$$\lambda_{\rm axi} \;=\; (2.03 \,\pm\, 0.02)\,{\rm cm}. \qquad (2)$$

The target heat flux in the (vacuum) RMP configuration, on the other hand, is characterized by a striation pattern which is guided by the perturbed separatrix with a maximal excursion of $L = 5.7\,{\rm cm}$. Within this domain, the averaged heat flux is characterized by a linear decay $\overline{q}_t \;=\; q_{t0}\,\left(1 \,-\, L/\mathcal{L}\right)$ with (see figure 5)

$$\mathcal{L}_{\rm RMP} \;=\; (7.91 \,\pm\, 0.16)\,{\rm cm}, \qquad (3)$$

while an exponential decay with $\lambda_{\rm RMP} \;=\; (2.25 \,\pm\, 0.05)\,{\rm cm}$ is found only in the far SOL (i.e. beyond $L = 5.7\,{\rm cm}$). A similar behavior is found for the plasma response case (with screening on the $m \,=\, 7 - 11$ surfaces), although the main strike point region is smaller ($L \,\approx\, 2.5\,{\rm cm}$). This region is characterized by a linear decay with

$$\mathcal{L}_{\rm m\,=\,7\text{-}11} \;=\; (4.74 \,\pm\, 0.09)\,{\rm cm}. \qquad (4)$$

An exponential decay is then again found in the far SOL with $\lambda_{m=7-11} \;=\; (2.10 \,\pm\, 0.04)\,{\rm cm}$.

III. CONCLUSIONS

We have investigated the impact of several uncertainties in 3D edge transport modeling of ITER similar shape plasmas at DIII-D. By applying an 'ad hoc' limit to the parallel electron heat conductivity we have shown that the flat temperature profile in the presence of RMPs is caused by fast parallel transport along open magnetic field lines. Furthermore, we have demonstrated that this limit has no impact on the target heat flux. We have shown, on the other hand, that the weak striation pattern of the target heat flux observed in low collisionality H-mode plasmas is may be related to (partial) screening of the externally applied RMP field, but not to a change in neutral gas pumping or impurity radiation (at least in this simple model). Finally, we have shown that the averaged target heat flux is broadened during RMP application with a linear decay in the main strike point region.

ACKNOWLEDGMENTS

This work was supported in part by the U.S. Department of Energy under DE-FC02-04ER54698.

REFERENCES

[1] Evans T E, *et al.*, 2004 *Phys. Rev. Lett.* **92** 23 235003. doi:10.1103/PhysRevLett.92.235003
[2] Liang Y, *et al.*, 2007 *Phys. Rev. Lett.* **98** 265004 1. doi:10.1103/PhysRevLett.98.265004
[3] Suttrop W, *et al.*, 2011 *Phys. Rev. Lett.* **106** 225004. doi:10.1103/PhysRevLett.106.225004
[4] Feng Y, *et al.*, 1997 *Journal of Nuclear Materials* **241-243** 930. doi:10.1016/S0022-3115(97)80168-7
[5] Feng Y, *et al.*, 2004 *Contrib. Plasma Phys.* **44** 1-3 57. doi:10.1002/ctpp.200410009
[6] Braginskii S, 1965 *Review of Plasma Physics* **1** 205
[7] Feng Y, *et al.*, 2006 *Nuclear Fusion* **46** 807. doi:10.1088/0029-5515/46/8/006
[8] Frerichs H, *et al.*, 2010 *Comp. Phys. Commun.* **181** 61. doi:10.1016/j.cpc.2009.08.016
[9] Frerichs H, *et al.*, 2011 *Phys. Plasmas* **(accepted)** "Impact of screening of resonant magnetic perturbations in 3D edge plasma transport simulations for DIII-D"
[10] Frerichs H, *et al.*, 2011 *Nuclear Fusion* **(accepted)** "On gas flow effects in 3D edge transport simulations for DIII-D plasmas with resonant magnetic perturbations"
[11] Frerichs H, *et al.*, 2010 *Nuclear Fusion* **50** 034004. doi:10.1088/0029-5515/50/3/034004
[12] Schmitz O, *et al.*, 2008 *Plasma Phys. Control. Fusion* **50** 124029. doi:10.1088/0741-3335/50/12/124029
[13] Cahyna P, *et al.*, 2011 *J. Nucl. Mater.* **415** S927. doi:10.1016/j.jnucmat.2011.01.117